Journal of Science: Advanced Materials and Devices 1 (2016) 343–350

Contents lists available at ScienceDirect

Journal of Science: Advanced Materials and Devices

journal homepage: www.elsevier.com/locate/jsamd

Original Article

FTIR and multivariate analysis to study the effect of bulk and nano copper oxide on peanut plant leaves

S. Suresh [a, b, *], S. Karthikeyan [c], K. Jayamoorthy [d]

[a] Research and Development Center, Bharathiar University, Coimbatore 641 046, Tamilnadu, India
[b] Department of Physics, St. Joseph's College of Engineering, Chennai 600 119, Tamilnadu, India
[c] Department of Physics, Dr. Ambedkar Government Arts College, Chennai 600 039, Tamilnadu, India
[d] Department of Chemistry, St. Joseph's College of Engineering, Chennai 600 119, Tamilnadu, India

ARTICLE INFO

Article history:
Received 26 July 2016
Accepted 12 August 2016
Available online 22 August 2016

Keywords:
Peanut plant
Copper oxide nanoparticles
FTIR
Multivariate analysis
Presoaking method

ABSTRACT

In this article the potential variation in biochemical constituents of peanut plant leaves affect by presoaking peanut seeds in copper oxide nanoparticles suspension has been studied and compared with its bulk counterpart. The synthesized nanoparticles were characterized by x-ray diffraction (XRD), scanning electron microscope (SEM) and transmission electron microscope (TEM) studies. The Fourier transform infrared (FTIR) analysis shows the most prominent peaks at ~2923 cm^{-1}, ~1636 cm^{-1} and ~1033 cm^{-1}, which correspond to lipids, protein and carbohydrate content in leaf samples respectively. The calculated mean ratio of the peak intensities for various frequency regions and total band area calculation for various band regions explain the variation in lipid, protein and carbohydrate content of leaf samples. Further the FTIR spectra were processed by de-convolution and curve fitting to quantitatively examine the chemical contents and structure changing of the secondary structure of protein. The calculated integrated band area of β − sheet, β − turn and α − helix secondary structure of protein varies to greater extent in all samples compared to control. Principal component analysis (PCA) has been carried out to explain the total variance in secondary structure of protein content in peanut plant leaves. Principal component 1 (PC1) accounts for 63.50% variation in secondary structure of protein whereas principal component 2 (PC2) accounts for 29.56%. The application of nanoparticles via presoaking method implies potential variation in biochemical constituents but doesn't affect the growth of plants considerably.

1. Introduction

Heavy metals are toxic to living organisms at elevated concentrations but it is more essential for many biochemical reactions. The elements essential for plants are classified as macronutrients (C, H, O, N, P, K, Ca, Mg, S) and micronutrients or trace elements (B, Cu, Fe, Mn, Mo and Zn). Lead and cadmium are the non-essential elements for any biochemical reaction or processes [1–3]. The micronutrients or trace elements are required for plants nutrition at micro level concentration but at higher concentrations affect the plants growth badly. Even though macronutrient required for plant growth, it becomes toxic when the concentration exceeds the permissible level. Copper (Cu) is an essential micronutrient involved in carbon assimilation and nitrogen metabolism; its deficiency results in severe growth retardation. Cu is also involved in lignin bio-synthesis, which not only provides strength to cell walls but also prevents wilting. Leaf chlorosis, stunted growth and stem and twig dieback are common symptoms of Cu deficiency [4]. Presoaking wheat seeds in Cu − EDTA solution (0.04–0.16 kg of copper per hectare (Cu ha^{-1})) substantially increased grain yield, but suppressed seedling emergence. Presoaking wheat seeds in Cu − EDTA solution at very low rates (0.04 kg Cu ha^{-1}) prevented Cu deficiency in wheat with significant increases in seed yield [4]. In another experiment on oats, seed presoaking with Cu (0.001% solution of $CuSO_4$) had no effect on germination; yet the number of grains (per panicle) and grain weight increased resulting in yield increase of 16.53% compared with untreated control [5]. Nowadays many works focus on application of nanoparticles in agriculture field. Nanoparticles gained considerable attraction because of their

* Corresponding author. Department of Physics, St. Joseph's College of Engineering, Chennai 600 119, Tamilnadu, India.
E-mail address: profsuresh1@gmail.com (S. Suresh).
Peer review under responsibility of Vietnam National University, Hanoi.

http://dx.doi.org/10.1016/j.jsamd.2016.08.004

unusual and fascinating properties, with various applications, over their bulk counterparts. Nanoparticles can serve as "magic bullets", containing herbicides, nano-pesticide fertilizers, or genes, which target specific cellular organelles in plant to release their content. In many works they are used to stimulate the seed germination and are used as a source of micronutrients [5–7].

Peanut (*Arachishypogaea*L.) contains rich oil and protein, and is an important oil source in processing industry. In some cases, peanut also serves as a supplementary food due to its high nutrition. They are extremely rich in vitamin B. They also stand out because of their high fat content and their huge amount of protein. Peanut is an important legume food crop of India grown in about 8 million ha of land. Peanut cultivation occurs in 108 countries around the world. The average productivity of peanut in India is around 1178 kg ha^{-1}, which is far less than the world's average 1400 kg ha^{-1}. The low productivity is mainly due to the fact that the crop is mostly grown in rain-fed, low fertility soils. Nanotechnology can present a solution to increase the value of agricultural products and environmental problems. With the using of nanoparticles and nanopowders, we can produce controlled or delayed releasing fertilizers [8]. Nanoparticles were high reactivity because of larger specific surface area, higher density of reactive areas, or increased reactivity of these areas on the particle surfaces. These features simplify the absorption of fertilizers and pesticides that are produced in nano scale. In this work the effect on biochemical constituents and metal concentration in peanut plant leaves (collected after 30 days of sowing), due to presoaking peanut seeds in copper oxide bulk and nanoparticle suspension for 10 h has been studied.

2. Experimental

2.1. Synthesis of nanoparticles

The copper oxide nanoparticle was synthesized using chemical precipitation method. Cupric nitrate is used as the precursor material and is taken as solution in a beaker. The cupric nitrate solution is stirred well using a magnetic stirrer and ammonium hydroxide solution is added in drops to form the copper hydroxide precipitate. The solution was continuously stirred to avoid agglomeration of precipitated particles. The precipitate is then washed several times with distilled water and ethanol further annealed at 400 °C for 4 h to remove water content and form copper oxide nanoparticles [9]. The annealed sample analyzed for phase confirmation and particle size using x-ray diffraction analysis (XRD), scanning electron microscope (SEM) and high resolution transmission electron microscope (HR-TEM) techniques [10].

2.2. Seed preparation and presoaking

The peanut seeds were obtained from Regional agricultural research institute, Virudhachalam. The seeds were sterilized in a 5% sodium hypochloride solution for 5–10 min, and then rinsed thoroughly several times with deionized water. The seeds were treated with two different concentration of copper oxide suspension (500 & 4000 ppm) of both nano and bulk for 10 hrs time period. Nanoparticle and bulk copper oxide suspensions were prepared by ultrasonification for 1 hr time period. Later the seeds sowed in separate pots for each concentration of both nano and bulk copper oxides. A total of three replicates were chosen for each morphological and physiological measurement (at an average of three plants per replica) where the results were presented as mean ± standard deviation (SD). Statistical significance was accepted when the probability of the result assuming the null hypothesis (p) is less than 0.05 (level of probability) [11–13].

2.3. FTIR spectral study

The leaf samples were sectioned from the plant collected after 30 days of sowing. All the leaf samples were oven dried at 100 °C for 48 hrs to remove moisture and ground to fine powder. The infrared spectra of leaves were recorded using KBr pellet technique in BRUKER IFS 66V model FTIR spectrometer in the region 4000–400 cm^{-1}. For each spectrum, 100 scans were co-added at a spectral resolution of ±4 cm^{-1}. The spectrometer was continuously purged with dry nitrogen. The frequencies for all sharp bands were accurate to 0.001 cm^{-1}. Each sample was scanned under the same conditions with three different pellets. These replicates were averaged and then used. Absorption intensity of the peaks was calculated by the base-line method. Special care was taken to prepare the pellets at the same thickness by taking the same amount of sample and applying the same pressure. Therefore, in the current study it is possible to directly relate the intensities of the absorption bands to the concentration of the corresponding functional groups. The spectra were analyzed using Origin 8.0 software (OriginLab Corporation, Massachusett, USA). For discussion the samples were named as L^1, L^2, L^3 and L^4 where, L^1 – Leaf samples of plant seeds soaked in 500 ppm copper oxide bulk suspension collected after 30 days of sowing, L^2 – Leaf samples of plant seeds soaked in 4000 ppm copper oxide bulk suspension collected after 30 days of sowing, L^3 – Leaf samples of plant seeds soaked in 500 ppm copper oxide nano suspension collected after 30 days of sowing, L^4 – Leaf samples of plant seeds soaked in 4000 ppm copper oxide nano suspension collected after 30 days of sowing.

2.4. Statistical analysis

All the statistical analysis was performed using SPSS 16.0 software. Pearson's correlation matrix was calculated for secondary structure protein and metal constituent variation in leaf samples. Principle component analysis was carried out to find the factors which influence the variation in protein content among the leaf samples treated with bulk and nano copper oxide in comparison with control sample. Graphical work was carried out using Origin software 8.0.

3. Results and discussion

3.1. XRD, SEM and TEM analyses of copper oxide nanoparticles

Fig. 1 visualizes the XRD pattern of copper oxide. The formation of copper oxide phase in 400 °C annealed sample was confirmed by an X-ray diffractometer. The average grain sizes were determined from the XRD patterns using the Debye-scherrer formula.

$$D = \frac{0.9^{*}\lambda}{\beta \cos\theta}$$

where D is the crystallite size, λ is the wavelength of Cu – $k\alpha_1 = 1.54060$ Å, β can be calculated from the experimental peak width (FWHM) of the most intense peak (0 0 2). The average particle size of the nanoparticle was found to be 28.45 nm. The peaks were matched using JCPDS software and it was well matched with the copper oxide (CuO) of file no "Pdf # 892531". Fig. 2 visualize the SEM image of copper oxide. The SEM image confirms the uniformity of phase formation and the particle size of the copper oxide nanoparticle. Fig. 3 shows the TEM image and selected area

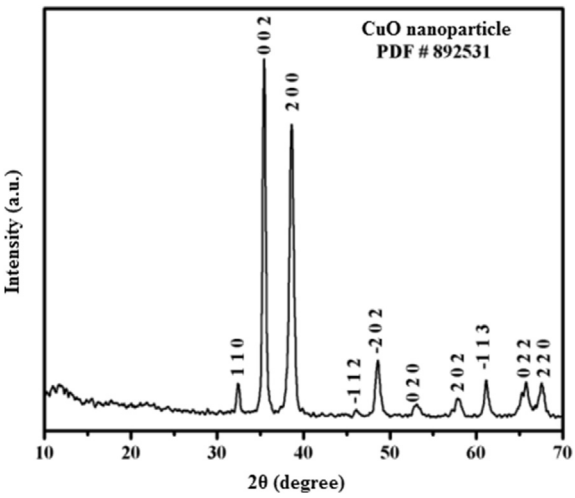

Fig. 1. XRD pattern of copper oxide nanoparticles.

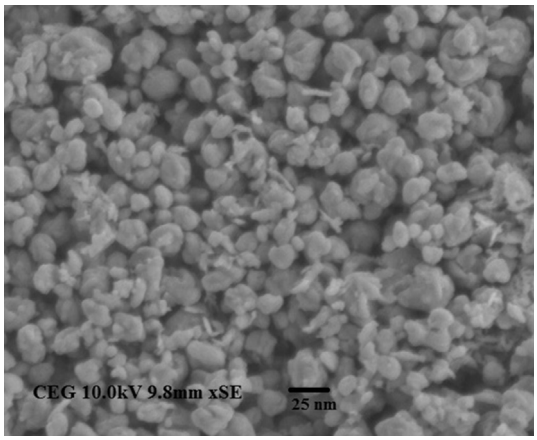

Fig. 2. SEM image of copper oxide nanoparticles.

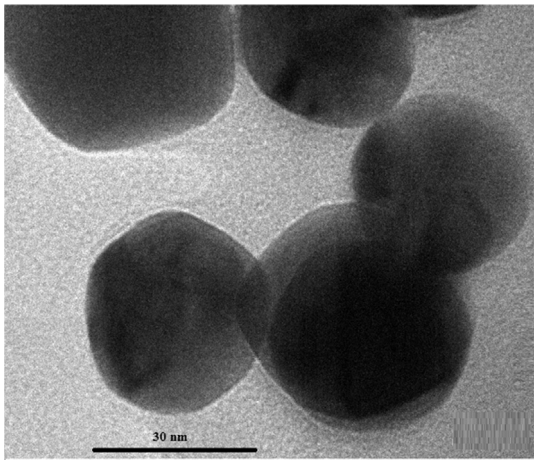

Fig. 3. TEM images of copper oxide nanoparticles.

electron diffraction (SAED) pattern of copper oxide nanoparticle. The image clearly shows the particle sizes are in nanometer and the SAED pattern explains the polycrystalline nature of copper oxide nanoparticle.

3.2. FTIR spectral studies of leaf samples

The tentative frequency assignment of averaged spectra for the peanut leaf samples collected after 30 days of sowing was tabulated in Table 1 and spectra shown in Fig. 4. The strong characteristic band at ~3404 cm^{-1} to ~3420 cm^{-1} in all the samples control, L^1, L^2, L^3 & L^4 is assigned to the O—H Stretching/N—H stretching of amide A. The CH_3 symmetric stretching band at ~2955 cm^{-1} in control sample was present in all the leaf samples however the intensity of L^1 sample found to be decreased attributed to weak bank at ~2955 cm^{-1}. The CH_2 symmetric stretching band and CH_2 asymmetric stretching of lipid, protein band at ~2921 cm^{-1} and ~2851 cm^{-1} respectively shows decreased intensity in all the leaf samples but L^2 leaf sample doesn't affect much compared to other leaf samples. The weak band at ~1736 cm^{-1} assigned to carbonyl C═O stretch: lipids, chlorophyll was found in leaf samples. The stretching vibration of free keto group at ~1725 cm^{-1} show elevated intensity in L^1 and L^2 samples but an 8 cm^{-1} shift was observed in all samples. The amide I protein is present in all the samples which was observed from the very strong band at ~1636 cm^{-1}. The band at ~1547 cm^{-1} gives the presence of amide II in all leaf samples but an increased intensity was found in L^2 sample alone might be due to the increase in overall protein content of leaf sample. There is no significant variation in bands at ~1426 cm^{-1}, ~1383 cm^{-1}, ~1255 cm^{-1} and ~1156 cm^{-1} in all leaf samples which shows there is no considerable variation in amide III protein and carbohydrates of these samples. The variation in intensities of bands from 1070 to 1033 cm^{-1} indicates the variation in carbohydrates and all other nucleic acids in L^1, L^3 and L^4 whereas there is no significant variation in L^2 sample. A very weak band at 962 cm^{-1} of C—N^+—C symmetric stretch of nuclei acids present in control sample alone and was absent in all other samples. The FTIR results show that the presoaking of peanut seeds with cuo bulk and nanoparticle suspensions of concentration 500 and 4000 ppm might have considerable influence on the protein, chlorophyll, carbohydrate and other biochemical constituents of leaf samples collected after 30 days of sowing. Many peaks were hidden in the raw FTIR spectra which can be unleashed by de-convolution and derivative spectra [14–16].

The total band area calculation for various spectral regions gives the changes in biochemical constituents of leaf samples directly from raw spectra. The spectral region between 3200 and 3450 cm^{-1} was selected to analyze amide A and B protein. The spectral region between 3000 and 2800 cm^{-1} was selected to analyze lipids. The spectral region between 1800 and 1500 cm^{-1} was selected to analyze proteins. The spectral region between 1450 and 1300 cm^{-1} was selected to analyze amide III protein. The spectral region between 1200 and 1000 cm^{-1} was selected to analyze carbohydrates [17].

Table 2 shows the total band area calculated for all the leaf samples control, L^1, L^2, L^3 & L^4. The total band area of the 3200–3450 cm^{-1} region increases in samples L^1, L^3 & L^4 but in L^2 sample it decreases by 8.78% compared to the control sample. This might be due to the decrease in amide-A protein in L^2 sample. The lipid content of leaf samples were analyzed by calculating the total band area in the region 2800–3000 cm^{-1}, which was found to decrease by 51.82%, 19.81% and 25.58% in L^1, L^3 & L^4 samples compared to control sample contrastingly the total band area was found to increase in L^2 by 6.85% attributed to slight increase in lipid content of L^2 sample. The amide I and amide II protein of leaf samples found to be increased in all the samples compare to control sample which was evidenced by the increase in total band area calculated for the region 1800–1500 cm^{-1}. The amide III protein, cellulose and lignin was estimated by the total band area calculated in the region 1300–150 cm^{-1} was found to decrease slightly in L^1, L^2

Table 1
Tentative frequency assignment of FTIR spectra for control, L^1, L^2, L^3 & L^4 leaf samples.

Control	Copper oxide bulk		Copper oxide nano		Tentative frequency assignment
	L^1	L^2	L^3	L^4	
3415 (vs)	3404 (vs)	3420 (vs)	3404 (vs)	3404 (vs)	Bonded O–H Stretching/N–H stretching, mainly due to Amide A protein
3347 (vs)	3384 (vs)	3365 (vs)	3366 (vs)	3365 (vs)	
2955 (m)	2955 (w)	2956 (m)	2956 (m)	2956 (m)	CH_3 symmetric stretching; lipid, protein
2921 (vs)	2921 (m)	2920 (s)	2919 (m)	2920 (m)	CH_2 asymmetric stretching; mainly lipid, protein
2851 (m)	2850 (w)	2850 (m)	2850 (w)	2850 (w)	CH_2 symmetric stretching; lipid, protein
1736 (w)	1734 (w)	1734 (w)	1735 (w)	1734 (w)	Carbonyl C=O stretch: lipids, chlorophyll
1725 (w)	1717 (m)	1717 (m)	1719 (w)	1717 (w)	Stretching vibration of free keto group, chl a
1630 (vs)	1636 (vs)	1635 (vs)	1639 (vs)	1636 (vs)	Amide I: C=O stretching of proteins, chlorophyll-water aggregates
1547 (m)	1541 (m)	1540 (s)	1535 (m)	1541 (m)	Amide II: N–H Bending/C–N stretching of proteins
1426 (m)	1419 (m)	1418 (m)	1425 (m)	1419 (m)	C–N stretching/in-plane OH bending
1383 (m)	1386 (m)	1385 (m)	1384 (m)	1385 (m)	CH_3 symmetric bending; protein
1255 (w)	1247 (w)	1260 (w)	1251 (w)	1248 (w)	C-0 stretching (ethers)/C–N stretching (amines)
1156 (m)	1152 (m)	1151 (w)	1152 (m)	1153 (m)	CH deformation, C–O, C–C stretching (carbohydrates)
1105(m)	1102(s)	1101(m)	1102(m)	1103(m)	
1070 (m)	1069 (s)	–	–	1071 (s)	PO_2^- symmetric stretch: mainly nucleic acids
1061 (m)	1061 (s)	1047 (m)	1062 (s)	1062 (s)	
1033 (m)	1034 (s)	1023 (m)	1035 (s)	1034 (s)	C–O stretching/C–O bending of the C–O–H carbohydrates
962 (vw)	–	–	–	–	$C–N^+–C$ symmetric stretch: nuclei acids

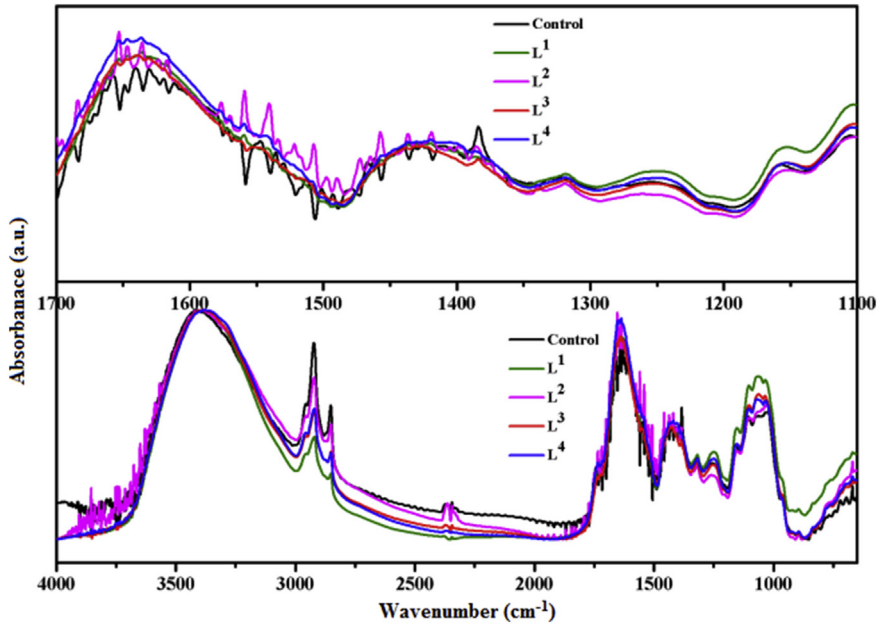

Fig. 4. FTIR spectra of control, L^1, L^2, L^3 & L^4 leaf samples.

Table 2
The total band area calculated for control, L^1, L^2, L^3 & L^4 leaf samples.

Spectral region (cm^{-1})	Control	L^1	L^2	L^3	L^4
3200–3450	409.92 ± 2.084	437.74 ± 0.150 +6.79	373.94 ± 0.864 −8.78	452.92 ± 1.026 +10.49	456.23 ± 2.052 +11.30
3000–2800	145.64 ± 0.841	70.17 ± 0.248 −51.82	155.61 ± 0.341 +6.85	116.79 ± 0.898 −19.81	108.37 ± 0.414 −25.58
1800–1500	135.35 ± 0.515	141.66 ± 0.481 +4.67	152.81 ± 1.015 +12.91	140.78 ± 0.980 +4.01	157.20 ± 0.180 +16.14
1300–1450	66.63 ± 0.478	65.21 ± 0.589 −2.12	62.72 ± 0.255 −5.86	72.30 ± 0.625 +8.52	65.93 ± 0.473 −1.05
1000–1200	96.02 ± 1.056	125.23 ± 0.840 +30.42	100.38 ± 0.634 +4.54	108.61 ± 0.756 +13.12	105.26 ± 0.314 +9.63

The values are the mean ± S.E for each group (n = 9). Comparisons were done by student t-test. The degree of significance was $p < 0.05$.

& L^4 samples but slightly increases in L^3 by 8.52%. The carbohydrates in all leaf samples found to be increased compared to control and highest variation was found in L^1 sample by 30.42% compared to control sample. On the whole the total band area calculations gives that there is considerable variation exists in proteins, lipid, carbohydrates, nuclei acids and other substances due to the pre-soaking of peanut seeds with copper oxide bulk and nano suspension.

The FTIR spectra were recorded with care by preparing the pellet of all the samples taking same weight during pelletizing, so the relative biochemical change is assessed by calculating the mean ratio of the peak intensities corresponding to various wavenumber. The mean ratio of the peak intensities of the bands at 1540 cm^{-1} and at 3347 cm^{-1} (I_{1540}/I_{3347}) was used as an indicator of the relative concentration of the protein in the leaf samples (Table 3). The calculated (I_{1540}/I_{3347}) ratio of L^1 and L^3 are 0.4816 ± 0.002 and 0.4336 ± 0.003 respectively which correspond to 9.89% and 18.88% decrease in relative protein over the control sample. On the other hand the relative protein found increased in L^2 and L^4 by 29.79% and 0.85% respectively with a mean intensity ratios of 0.6937 ± 0.003 and 0.5390 ± 0.005. The mean ratios of the absorption intensity of the methyl band and methylene band (I_{2954}/I_{2850}) of samples L^1, L^2, $L^3$and L^4 are 1.2948 ± 0.011, 1.0647 ± 0.006, 1.1745 ± 0.008 and 1.2254 ± 0.009 respectively, which correspond to an increase of 28.25%, 5.45%, 16.33% and 21.37% respectively. The increase in the ratios indicates the number of methyl groups in protein fibers is more compared to methylene groups in these leaf samples [17–19].

The mean ratio of the intensities of the bands at 1540 cm^{-1} and 1635 cm^{-1} could be attributed to change in the composition of the whole protein pattern. The calculated mean ratio of intensities of L^1, L^3 and L^4 samples are 0.5350 ± 0.002, 0.4868 ± 0.002 and 0.5552 ± 0.001, which attribute to the decrease in whole protein of 13.97%, 21.73%, and 10.73% in these samples respectively. The L^2 sample of leaves shows 15.11% increase in total protein which indicates the seeds soaked in 4000 ppm of copper oxide bulk suspension increases the total protein content. From these results it was observed that the total protein of leaf samples affect more positively when seeds presoaking in 500 ppm concentration of bulk and nano copper oxide suspension compared to higher concentration of 4000 ppm suspension.

The mean ratio of peak intensities of the bands (I_{1071}/I_{1540}) is found to be 1.4740 ± 0.004, 0.8411 ± 0.002, 1.4688 ± 0.007 and 1.1436 ± 0.003 for L^1, L^2, L^3 and L^4 respectively. The glycoprotein of L^1, L^3 and L^4 leaf samples increased by 40.50%, 40.00%, and 9.01% respectively, whereas L^2 sample exhibit decrease of 19.83%. The lipid, chlorophyll variation was analyzed from the calculated mean ratio of peak intensities of the bands (I_{1734}/I_{1430}), the values are 0.6386 ± 0.009, 0.7570 ± 0.008, 0.5640 ± 0.005 and 0.6603 ± 0.006 for L^1, L^2, L^3 and L^4 leaf samples. The results shows a decrease of 6.06% and 13.68% in L^1 and L^3 leaf samples respectively but an increase of 15.84% and 1.05% increase in L^2 and L^4 leaf samples compared to the control value of 0.9071 ± 0.009. The increase in ratio suggested that lipids are being oxidized in L^2 sample. Since oxidation can cause an increase in carbonyls and a degradation of lipids, both of these changes could be contributed to the elevated ratio which in turn affects the chlorophyll. The mean ratio of peak intensities of bands (I_{1734}/I_{1540}) and (I_{1430}/I_{1540}) of L^2 sample decreased when compared to the control leaf sample, suggesting that lipid degradation predominates over carbonyl formation whereas it found to be increased in L^1, L^3 and L^4 leaf samples.

FTIR spectroscopy is one of the major techniques for the determination of protein secondary structures. The Fourier self-deconvolution and second derivative spectra could explain more details about the impact of bulk and nano copper oxide suspension on peanut plant leaves. To study the secondary structure of proteins in the leaf samples, further analysis has been carried out by resolving the amide I band using the curve fitting method. To find out the number of peaks in the amide I region for curve-fitting process, the second derivative spectra were calculated using Origin 8.0 software (Savitsky–Golay as a derivative operation) in the amide I region. The derivatives gave the number and positions, as well as an estimation of the bandwidth and intensity of the bands making up the amide I region. After baseline correction, the best fit for decomposing the amide I bands in the spectral region of interest was obtained by Gaussian components using the same software. The underlying bands of amide I band as deduced by curve-fitting analysis for the control, and samples treated with various concentration of bulk and nano copper oxide were tabulated in Table 4. The band around 1633 cm^{-1} is assigned for β − sheet of secondary structure of protein and its integrated band area is found to increase in L^1 and L^2 leaf samples by 1.31% and 20.29% respectively but found to decrease in L^3 and L^4 samples by 41.33% and 39.63% respectively. This indicates the peanut seeds soaked in copper oxide nanoparticle suspension show a decrease in β − sheet of secondary structure of protein whereas it increased in copper oxide bulk suspension. The random coil of the secondary structure of protein was observed from the peak centered at 1648 shows increase in band area of all the samples considerably expect L^4 sample where it found decrease by 12.86%. The band at 1656 is due to α − helix of secondary protein structure which shows a steep increase in band area of 200.37%, 65.40, 125.48% and 164.11% in L^1, L^2, L^3 and L^4 samples respectively. The bands centered around 1666, 1673 and 1684 were assigned for the β − turn of the secondary protein structure (Table 4). The integrated band area for 1666 is found to decrease in L^3 sample by 38.92%, whereas it was increased in all other samples. The integrated band area of 1673 and 1684 were increased in all the leaf samples. The percentage variation in band area of β − sheet, β − turn and α − helix of secondary structure of protein might be due to the interaction of peanut seeds with copper oxide bulk and nanoparticles [20,21].

Table 3
Mean ratio of peak intensities of the bands at different wave numbers.

Ratio of bands	Control	L^1	L^2	L^3	L^4
I_{1540}/I_{3347}	0.5345 ± 0.001	0.4816 ± 0.002 −9.89	0.6937 ± 0.003 +29.79	0.4336 ± 0.003 −18.88	0.5390 ± 0.005 +0.85
I_{2954}/I_{2850}	1.0096 ± 0.002	1.2948 ± 0.011 +28.25	1.0647 ± 0.006 +5.45	1.1745 ± 0.008 +16.330	1.2254 ± 0.009 +21.37
I_{1540}/I_{1635}	0.6219 ± 0.008	0.5350 ± 0.002 −13.97	0.7159 ± 0.005 +15.11	0.4868 ± 0.002 −21.73	0.5552 ± 0.001 −10.73
I_{1071}/I_{1540}	1.0491 ± 0.004	1.4740 ± 0.004 +40.50	0.8411 ± 0.002 −19.83	1.4688 ± 0.007 +40.00	1.1436 ± 0.003 +9.01
I_{1734}/I_{1430}	0.6535 ± 0.007	0.6386 ± 0.009 −6.06	0.7570 ± 0.008 +15.84	0.5640 ± 0.005 −13.68	0.6603 ± 0.006 +1.05
I_{1734}/I_{1540}	0.6178 ± 0.003	0.6375 ± 0.004 +3.20	0.5725 ± 0.003 −7.32	0.6414 ± 0.012 +3.83	0.6289 ± 0.003 +1.80
I_{1430}/I_{1540}	0.9453 ± 0.002	1.0386 ± 0.007 +9.86	0.7563 ± 0.001 −19.99	1.1372 ± 0.009 +20.29	0.9523 ± 0.006 +0.74

The values are the mean ± S.E for each group (n = 9). Comparisons were done by student t-test. The degree of significance was $p < 0.05$.

Table 4
Frequency assignment for secondary protein obtained by self deconvoluted spectra.

Wavenumber (cm^{-1})	Control	L^1	L^2	L^3	L^4
1633 (β − sheet)	1.4785 ± 0.002	1.4978 ± 0.005 +1.31	1.7784 ± 0.002 +20.29	0.8674 ± 0.004 −41.33	0.8926 ± 0.004 −39.63
1648 (Random coil)	2.2533 ± 0.004	3.7506 ± 0.008 +66.45	2.7740 ± 0.005 +23.11	2.4114 ± 0.007 +7.02	1.9635 ± 0.002 −12.86
1656 (α − helix)	1.0347 ± 0.006	3.1078 ± 0.001 +200.37	1.7113 ± 0.004 +65.40	2.3329 ± 0.003 +125.48	2.7327 ± 0.004 +164.11
1666 (β − turn)	1.3915 ± 0.006	3.6970 ± 0.002 +165.69	1.6319 ± 0.006 +17.28	0.8500 ± 0.007 −38.92	2.1345 ± 0.001 +53.40
1673 (β − turn)	0.9997 ± 0.008	1.9707 ± 0.006 +97.14	3.1976 ± 0.006 +219.87	1.6977 ± 0.004 +69.82	1.9068 ± 0.002 +90.74
1684 (β − turn)	2.1776 ± 0.007	2.7620 ± 0.009 +26.84	2.6755 ± 0.003 +22.87	2.2840 ± 0.009 +4.89	3.6277 ± 0.003 +66.59

The values are the mean ± S.E for each group (n = 9). Comparisons were done by student t-test. The degree of significance was $p < 0.05$.

3.3. Pearson correlation coefficient matrix for secondary structure of protein

The Pearson's correlation coefficient matrix measures the strength of a linear relationship between any two variables on a scale of +1 (positive linear correlation) to −1 (negative linear correlation). In this study, the derived intensities of the secondary structure protein were used in calculating the correlation coefficient using the SPSS 16.0. The matrix of linear correlation coefficient is shown in Table 5 which is significant at the 0.01 level (2-tailed). The correlation coefficient values vary from 0.709 between 1633 and 1648, to 0.990 between 1656 and 1673. The results shows that positive correlation exist between 1633 and 1656, 1656–1673 and 1656–1684 which clearly indicates α − helix increases with increase in β − sheet and β − turn vice versa. A positive correlation exist between the wavenumber corresponds to 1673 and 1684 assigned to β − turn of secondary structure of protein. There is no negative correlation between any of the secondary structures of protein which indicates α − helix; β − sheet and β − turn does not increase at the expenses of one another [22].

3.4. Principal component analysis for variation in secondary structure of protein

Further principal component analysis using SPSS 16.0 software is performed for understanding the protein secondary structure variation among the samples treated with bulk and nano copper oxide compared with control sample. The results in Table 6 shows that the variation of secondary structure of protein due to the metal treatment is calculated using varimax rotated factor analysis of principal component extraction method.

Using rotated factor loading and commonalities varimax rotation analysis, information about the main factors in the studied samples was obtained. The successive factors account for decreasing amounts of residual variance using two factors (varimax rotation) for the samples Control, L^1, L^2, L^3 and L^4 of leaf samples. The main factor (>0.6) for L^1, L^2 and L^4 is noted as factor 1. Factor 2 contributes control & L^3. Factor analysis or principle component analysis is a useful tool in the examination of multivariate data (Fig. 5). The cumulative percentage of explained variance in secondary structure of protein of all leaf samples is 93.051%. Factor 1 account for 63.496% of the total data variance so the variation of secondary structure of protein was established by accounting the L^1, L^2 and L^4 samples. Factor 2 accounts for 29.555% which includes the control and L^3 samples. Fig. 6 shows the PC loadings plot for the spectral range 1600–1700 cm^{-1} which clearly shows the PC1 factor might establish the maximum variation of the secondary structure of protein in leaf samples compared to other component.

Table 5
Pearson correlation matrix for variation in secondary structure protein of control, L^1, L^2, L^3 & L^4 leaf samples.

Wavenumber (cm^{-1})	1633	1648	1656	1666	1673	1684
1633	1	0.709	0.968[a]	0.927[b]	0.926[b]	0.941[b]
1648	0.709	1	0.853	0.712	0.888[b]	0.814
1656	0.968[a]	0.853	1	0.945[b]	0.990[a]	0.981[a]
1666	0.927[b]	0.712	0.945[b]	1	0.950[b]	0.987[a]
1673	0.926[b]	0.888[b]	0.990[a]	0.950[b]	1	0.987[a]
1684	0.941[b]	0.814	0.981[a]	0.987[a]	0.987[a]	1

[a] Correlation is significant at the 0.01 level (2-tailed).
[b] Correlation is significant at the 0.05 level (2-tailed).

Table 6
Variation of metal concentration in leaf samples of control, L^1, L^2, L^3 and L^4 is calculated using varimax rotated factor analysis of principal component extraction method.

Component	Rotation sums of squared loadings		
	Total	% of variance	Cumulative %
1	3.175	63.496	63.496
2	1.478	29.555	93.051

Rotated component matrix

Samples	Component	
	1	2
Control	−0.695	0.700
L^1	0.980	−0.057
L^2	0.889	0.015
L^3	0.091	0.988
L^4	0.966	−0.087

4. Conclusions

The effect of presoaking peanut seeds in bulk and nano form of copper oxide suspension is studied extensively. The synthesized copper oxide nanoparticle was phase confirmed with XRD results and it measures average particle size of 28.45 nm. The SEM, TEM and AFM image confirms the uniformity and particle size of nanophase throughout the sample. The FTIR results of peanut plant leaves collected after 30 days of growth period suggest the copper oxide nanoparticle has considerable effect when applied through presoaking the peanut plant seeds in copper oxide bulk and nanoparticle suspensions. The FTIR results shows that the presoaking of peanut seeds with copper bulk and

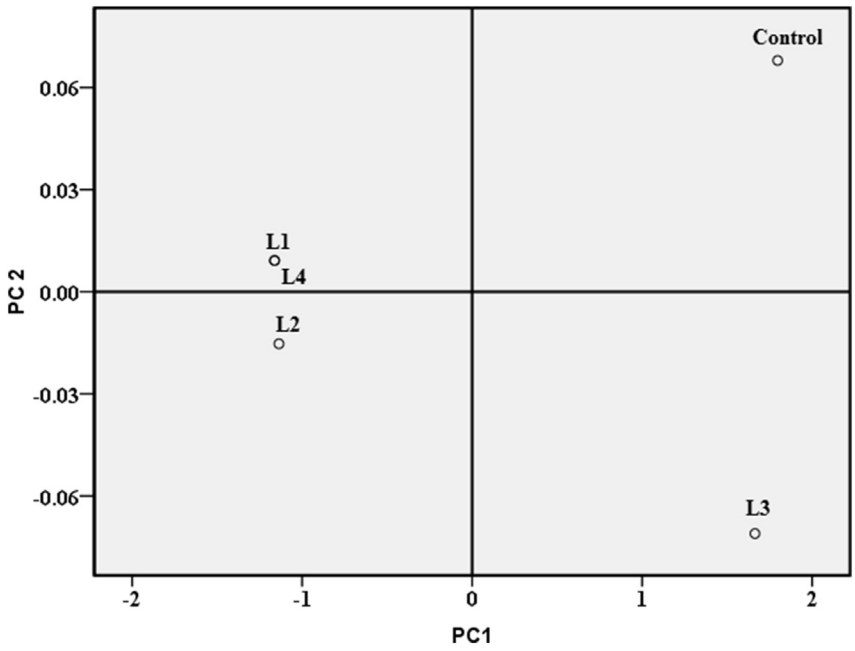

Fig. 5. Principle component analysis explained variance in secondary structure protein of control, L^1, L^2, L^3 & L^4 leaf samples.

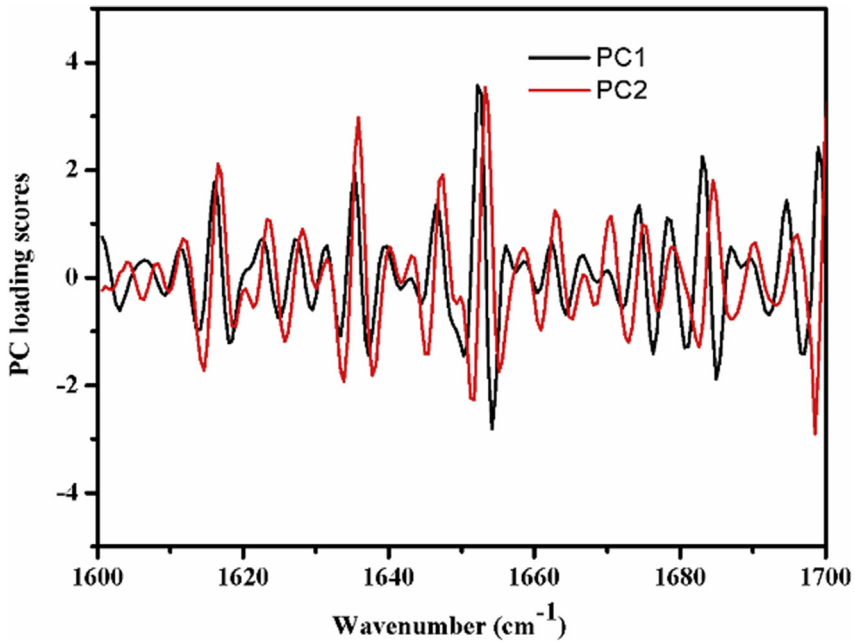

Fig. 6. PC loadings plot for the spectral range 1600–1700 cm^{-1}.

nanoparticle suspensions of concentration 500 and 4000 ppm might have considerable influence on the protein, chlorophyll, carbohydrate and other biochemical constituents of leaf samples collected after 30 days of sowing. The band area results of β − sheet, β − turn and α − helix of secondary structure of protein varies to greater extent in all samples compared to control. The correlation matrix for secondary structures of protein shows that variation in α − helix plays a major role in secondary structure protein variation of leaf samples. The PCA analysis suggests that L^1, L^2 and L^4 samples explains the total variance of the secondary structure of protein content in leaf samples of peanut plant.

References

[1] B.J. Alloway, Heavy Metals in Soils, Blackie & Sons, Glasgow, 1990, pp. 284–305. UK.
[2] N.C. Brady, R.R. Weil, The Nature and Properties of Soils, 14th ed., 2008 (Practice-Hall, New Jersey, USA).
[3] L. Taiz, E. Zeiger, Plant Physiology, fifth ed., Sinauer Associates, Inc., Publishers, Sunderland, MA, USA, 2010.
[4] S.S. Malhi, Effectiveness of seed-soaked Cu, autumn- versus spring-applied Cu, and Cu-treated P fertilizer on seed yield of wheat and residual nitrate-N for a Cu-deficient soil, J. Plant Sci. 89 (2009) 1017–1030.
[5] S. Suresh, S. Karthikeyan, K. Jayamoorthy, Effect of bulk and nano-Fe_2O_3 particles on peanut plant leaves studied by Fourier transform infrared spectral studies, J. Adv. Res. (2015), http://dx.doi.org/10.1016/j.jare.2015.10.002.

[6] P. Saravanan, K. Jayamoorthy, S.A. Kumar, Switch-On fluorescence and photo-induced electron transfer of 3-aminopropyl triethoxysilane to ZnO: dual applications in sensors and antibacterial activity, Sensors Actuators B Chem. 221 (2015) 784–791.
[7] S. Suresh, K. Jayamoorthy, P. Saravanan, S. Karthikeyan, Switch-Off fluorescence of 5-amino-2-mercapto benzimidazole with Ag_3O_4 nanoparticles: experimental and theoretical investigations, Sensors Actuators B 225 (2016) 463–468.
[8] Anonymous, Nano technology in agriculture, J. Agric. Technol. 114 (2009) 54–65 (In Persian).
[9] Kankanit Phiwdang, Sineenart Suphankij, Wanichaya Mekprasart, Wisanu Pecharapa, Synthesis of CuO nanoparticles by precipitation method using different precursors, Energy Procedia 34 (2013) 740–745.
[10] S. Suresh, P. Saravanan, K. Jayamoorthy, S. Ananda Kumar, S. Karthikeyan, Development of silane grafted ZnO core shell nanoparticles loaded diglycidyl epoxy nanocomposites film for antimicrobial applications, Mater. Sci. Eng. C 64 (2016) 286–292.
[11] B. Abdulrahmani, K. Ghassemi-Golezani, M. Valizadeh, V. Feizi-Asl, Seed priming and seedling establishment of barley (Hordeum vulgare L.), J. Food Agri. Environ. 5 (2007) 179–184.
[12] T. Saric, B. Saciragic, Effect of oat seed treatment with microelements, Plant Soil 31 (1969) 185–187.
[13] L. Zheng, F.S. Hong, S.P. Lu, C. Liu, Effect of nano-TiO2 on strength of naturally aged seeds and growth of spinach, Biol. Trace Elem. Res. 104 (2005) 83–91.
[14] X.M. Tan, C. Lin, B. Fugetsu, Studies on toxicity of multiwalled carbon nanotubes on suspension rice cells, Carbon 47 (2009) 3479–3487.
[15] T.N.V.K.V. Prasad, P. Sudhakar, Y. Sreenivasulu, P. Latha, V. Munaswamy, K. Raja Reddy, T.S. Sreeprasad, P.R. Sajanlal, T. Pradeep, Effect of nanoscale zinc oxide particles on the germination, growth and yield of peanut, J. Plant Nutr. 35 (2012) 905–927.
[16] S. Sukhdev, D. Malhi, Leach, reducing toxic effect of seed-soaked Cu fertilizer on germination of wheat, Agric. Sci. 3 (2012) 674–677.
[17] P.L.R.M. Palaniappan, T. Nishanth, V.B. Renju, Bioconcentration of zinc and its effect on the biochemical constituents of the gill tissues of Labeo rohita: an FTIR study, Infrared Phys. Technol. 53 (2010) 103–111.
[18] B. Rao Adari, S. Alavala, Sara A. George, H.M. Meshram, A.K. Tiwari, V.S. Akella, S. Sarma, Synthesis of rebaudioside-A by enzymatic transglycosylation of stevioside present in the leaves of Stevia rebaudiana Bertoni, Food Chem. 200 (2016) 154–158.
[19] M. Mecozzi, M. Pietroletti, R.D. Mento, Application of FTIR spectroscopy in ecotoxicological studies supported by multivariate analysis and 2D correlation spectroscopy, Vib. Spectrosc. 44 (2007) 228–235.
[20] G. Cakmak, I. Togan, F. Severcan, 17Beta-estradiol induced compositional, structural and functional changes in rainbow trout liver, revealed by FTIR spectroscopy: a comparative study with nonylphenol, Aquat. Toxicol. 77 (2006) 53–63.
[21] S. Suresh, K. Jayamoorthy, S. Karthikeyan, Fluorescence sensing of potential NLO material by bunsenite NiOnanoflakes: room temperature magnetic studies, Sensors Actuators B 232 (2016) 269–275.
[22] S. Suresh, S. Karthikeyan, K. Jayamoorthy, Spectral investigations to the effect of bulk and nano ZnO on peanut, Karbala Int. J. Mod. Sci. 2 (2016) 69–77.